

Phase Separation and Magnetic Properties of Half-metal-type $\text{Co}_2\text{Cr}_{1-x}\text{Fe}_x\text{Al}$ Alloys

著者	石田 清仁
journal or publication title	Applied Physics Letters
volume	85
number	20
page range	4684-4686
year	2004
URL	http://hdl.handle.net/10097/34886

Phase separation and magnetic properties of half-metal-type $\text{Co}_2\text{Cr}_{1-x}\text{Fe}_x\text{Al}$ alloys

K. Kobayashi,^{a),b)} R. Y. Umetsu,^{a)} R. Kainuma,^{a)} K. Ishida,^{a)} T. Oyamada, A. Fujita, and K. Fukamichi

Department of Materials Science, Graduate School of Engineering, Tohoku University, Aoba-yama 6-6-02, Sendai 980-8579, Japan

(Received 8 June 2004; accepted 16 September 2004)

The phase stability and magnetic properties of the half-metal-type $\text{Co}_2\text{Cr}_{1-x}\text{Fe}_x\text{Al}$ alloy system were investigated. It was found that the occurrence of two-phase separation is unavoidable in a concentration range of less than $x=0.4$, leading to deviation of the saturation magnetic moments from the generalized Slater–Pauling line. The $L2_1$ -type phase becomes stable in a concentration range of more than $x=0.7$, where no half-metallic behaviors are present. Consequently, it is concluded that the most favorable concentration for applications to spintronic devices is located around $x=0.4$ in $\text{Co}_2\text{Cr}_{1-x}\text{Fe}_x\text{Al}$ alloys having the $B2$ -type phase. © 2004 American Institute of Physics. [DOI: 10.1063/1.1821654]

Half-metallic ferromagnets (HMFs) have been investigated intensively in the field of spintronics in order to realize spin-dependent devices with high performance. HMFs having a complete (=100%) spin-polarization were first pointed out by de Groot *et al.* from the band calculations for the Cl_b (half-Heusler)-type alloys of NiMnSb and PtMnSb.¹ Subsequently, many $L2_1$ (full-Heusler)-type HMFs have been investigated extensively from both theoretical and experimental viewpoints.^{2–7}

From theoretical calculations,^{8–12} it has been reported that $L2_1$ and $B2$ -type $\text{Co}_2\text{Cr}_{1-x}\text{Fe}_x\text{Al}$ alloys exhibit half-metal-type band structures in the lower concentration range of x . Inomata *et al.* have demonstrated that the magnetic tunneling junctions using $B2$ -type $\text{Co}_2\text{Cr}_{1-x}\text{Fe}_x\text{Al}$ alloys with $x=0.4$ exhibit a large value of tunneling magnetoresistance of 19% at room temperature.^{13,14} Compared with the expected value,^{10–12} however, this value is significantly low. Furthermore, the saturation magnetic moment at 4.2 K for Co_2CrAl alloy has been reported to be $1.55 \mu_B/\text{f.u.}$,¹⁵ which is about half the value obtained from the generalized Slater–Pauling line of $M_t = Z_t - 24$.^{5,16} Here, M_t and Z_t represent the total spin magnetic moment per unit cell and the total number of valence electrons, respectively. Theoretically, the reductions of the spin polarization and the saturation magnetic moment mentioned above for the Co_2CrAl alloy were associated with the disordering between the Co and Cr sites.^{10,11} However, it has become clear that the disordering between the Co and Cr sites is unlikely to occur energetically.^{10,11} Experimentally, no investigations on the phase stability of $\text{Co}_2\text{Cr}_{1-x}\text{Fe}_x\text{Al}$ alloy system have been conducted. Accordingly, it is still unclear what does affect the half-metallic properties of the $\text{Co}_2\text{Cr}_{1-x}\text{Fe}_x\text{Al}$ alloys. Therefore, in the present study, we carried out the metallurgical observations in order to discuss the phase stability. Furthermore, the magnetic properties which reflected the phase stability were measured for both the $B2$ and $L2_1$ -type $\text{Co}_2\text{Cr}_{1-x}\text{Fe}_x\text{Al}$ alloys.

Several kinds of the specimens were prepared by arc-melting or in an induction furnace under an argon gas atmosphere. After alloying, each ingot was annealed at 1373 K for 72 h and quenched in ice water. Additional annealings at various temperatures were done for some specimens. The compositions of the specimens were determined with an electron probe microanalyzer. Identifications of their structure and the phase were achieved by electron diffraction and transmission electron microscopic (TEM) observations. The phase transformation temperature was determined by differential scanning calorimetry (DSC) measurements. Magnetic measurements were carried out with a superconducting quantum interference devices magnetometer and a vibrating sample magnetometer. The value of magnetization was calibrated by using a pure Ni metal.

Figures 1(a)–1(c) show the selected area diffraction patterns with the specimen tilted to the $[01\bar{1}]$ matrix zone axis and TEM dark-field images taken from the $(100)_{B2}$, $(200)_{L2_1}$, or $(111)_{L2_1}$ reflections for $\text{Co}_2\text{Cr}_{1-x}\text{Fe}_x\text{Al}$ alloys with $x=0.0$, 0.5, and 1.0. The alloys with $x=0.0$ (a) and 0.5 (b) were prepared by annealing at 773 K for 72 h and the alloy with $x=1.0$ (c) was obtained by annealing at 873 K for 168 h. The single- and double-headed arrows for the dark-field images in (b) indicate the same area of the $A2$ -type phase. Note that a blank panel in Fig. 1 is unnecessary because the (111) plane is absent in the $B2$ phase. From the electron diffraction patterns, two-phase separation is confirmed in Figs. 1(a) and 1(b) for the TEM observations, although the crystal structure of (a) is identified as the $B2$ -type and that of (b) and (c) as the $L2_1$ -type. In the TEM dark-field image for (a), the dark and white regions correspond to the $A2$ - and $B2$ -type phases, respectively. For the TEM dark-field images of (b), the two-phase separation of the $A2$ - and $L2_1$ -type phases is confirmed. It is suggested by our thermodynamical calculations that the metastable equilibrium compositions of the $B2$ and the $A2$ phases shift to CoAl-rich and CoCr-rich phases, respectively.¹⁷ In the TEM dark-field image for (c), the antiphase boundary of the $L2_1$ phase without any precipitates can be observed.

A metastable phase diagram of the $\text{Co}_2\text{Cr}_{1-x}\text{Fe}_x\text{Al}$ alloy system is presented in Fig. 2. The solid line gives the bound-

^{a)}Also at: Core Research for Evolutional Science and Technology, Japan Science and Technology Agency.

^{b)}Author to whom correspondence should be addressed; electronic mail: kosei@material.tohoku.ac.jp

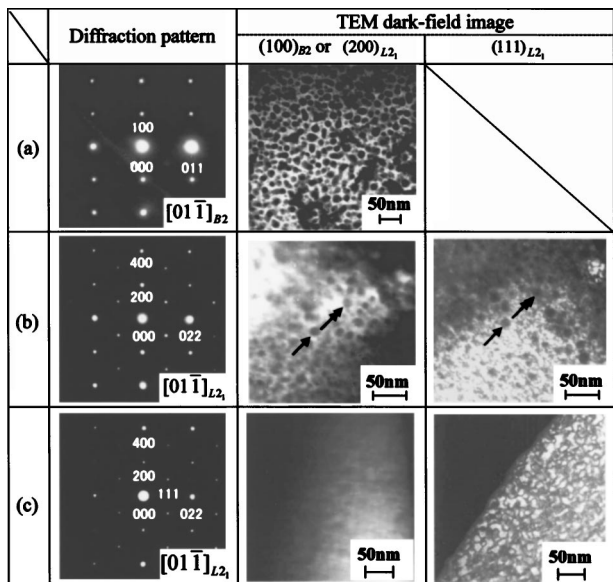


FIG. 1. Selected area diffraction patterns of the specimen tilted to the [011] matrix zone axis and TEM dark-field images taken from the (100)_{B2}, (200)_{L21}, or (111)_{L21} reflection for Co₂Cr_{1-x}Fe_xAl alloys with $x = 0.0, 0.5, \text{ and } 1.0$. (a) $x = 0.0$ annealed at 773 K for 72 h, (b) $x = 0.5$ annealed at 773 K for 72 h, (c) $x = 1.0$ annealed at 873 K for 168 h. Single- and double-headed arrows in the dark-field images of the Co₂Cr_{0.5}Fe_{0.5}Al alloy indicate the same area of the A2-type phase.

ary between the single-phase region and the two-phase region. The dashed line depicts the transformation temperature between the L_{21} phase and the B_2 phase. The temperatures represented by the closed circles and the diamonds were decided from the DSC measurements. Although the B_2 phase exists at higher temperatures in all concentration ranges, the occurrence of two-phase separation is unavoidable in the lower concentration range of x . In the alloy with $x = 0.4$, the single phase of B_2 phase is obtainable at room temperature by quenching from 1173 K. On the other hand, in the alloy with less than $x = 0.4$, two-phase separation inevitably takes place regardless of the heat treatment conditions. After obtaining a B_2 -type single phase more than $x = 0.7$, the L_{21} -type single phase is obtainable after heat treatment.

From the thermomagnetization curves for a heating rate of 1.6 K/min, the Curie temperature T_C of the B_2 phase

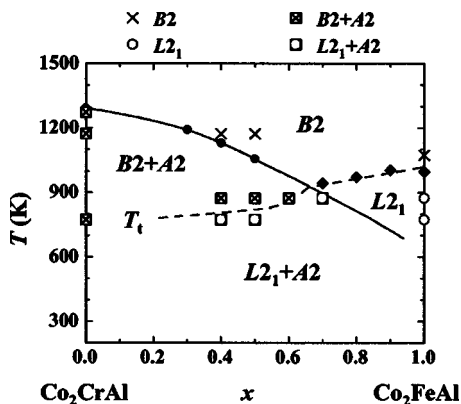


FIG. 2. Metastable phase diagram of the Co₂Cr_{1-x}Fe_xAl alloy system. The solid line gives the boundary between the single-phase region and the two-phase region. The dashed line represents the transformation temperature T_t between the B_2 and L_{21} phases. The temperatures represented by the closed circles and diamonds are determined based on the DSC measurements.

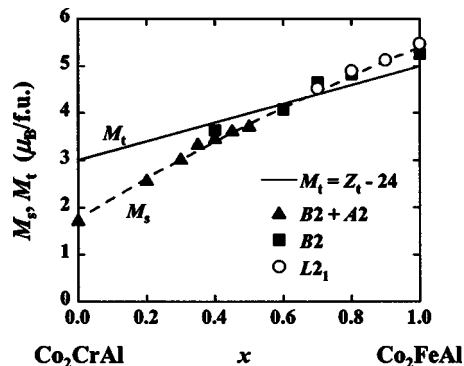


FIG. 3. Concentration dependence of the saturation magnetic moments M_s for Co₂Cr_{1-x}Fe_xAl alloys. The closed circles and triangles stand for M_s for the $B_2 + A_2$ and the B_2 phases, respectively. The open squares represent M_s of the L_{21} phase. The solid line gives the generalized Slater–Pauling line (Refs. 5,15).

alloy with $x = 0.5$ is about 850 K, and that of the L_{21} phase alloys with $x = 0.8$ and 1.0 is 1041 and 1170 K, respectively. Therefore, T_C increases with increasing x . However, it should be noted that these values would change, depending on the measuring conditions. For example, the phase separation and the degree of order are affected by the heating rate.¹⁸

The concentration dependence of the saturation magnetic moments M_s measured at 4.2 K for Co₂Cr_{1-x}Fe_xAl alloys is shown in Fig. 3. The closed triangles and squares stand for M_s of the $B_2 + A_2$ and the B_2 phases, respectively. The open circles represent M_s of the L_{21} phase and the solid line gives the generalized Slater–Pauling line of $M_t = Z_t - 24$. The formula unit of the B_2 phase is twice that of the L_{21} phase. The deviation of M_s from the solid line becomes significant in the lower concentration range of x . This is due to the two-phase separation. The systematic theoretical calculations for Co₂Cr_{1-x}Fe_xAl alloy system indicate that the atomic disordering between the Co and (Cr, Fe) sites degrades the half-metallic properties, leading to the reduction of the spin polarization and the magnetic moment.^{10,11} The possibility of degradation of the half-metallic properties of Co₂Cr_{1-x}Fe_xAl alloy system has also been theoretically discussed by considering the atomic disordering between the (Cr, Fe) and Al sites, but it has no marked effects on the half-metallic properties.^{10,11} Furthermore, it has been reported that the magnetic moment of the B_2 phase for Co₂Cr_{1-x}Fe_xAl alloys is almost the same as that of the L_{21} phase,^{11,12} and the L_{21} and the B_2 phases of Co₂Cr_{1-x}Fe_xAl alloys with higher concentration of x no longer exhibit half-metallic properties in their band structures.⁹⁻¹² In addition, the two-phase separation results in heterogeneity in the specimen as discussed in connection with Fig. 2.

More noteworthy is that the calibrated value of M_s for the alloy with more than $x = 0.7$ is rather larger than that of the solid line of $M_t = Z_t - 24$. It should be noted that the generalized Slater–Pauling line often underestimates the experimental magnetic moments of the various transition metal alloys and compounds.¹⁶ In several Co-based Heusler alloy systems, it has been pointed out from XMCD measurements that the magnitude of the orbital magnetic moment is relatively large, being about 5%–10% of the spin magnetic moment.¹⁹⁻²¹ Therefore, it is expected that the present larger value of the magnetic moment is explained as the contribution from the orbital magnetic moment. On the other hand,

recent theoretical studies including the spin-orbit coupling have shown that the orbital magnetic moments for the Heusler alloys are negligibly small^{22,23} since the symmetry of the cubic lattice of the Heusler alloys is very high, and then the magnetic anisotropy is very small. Further investigations are necessary to clarify the difference in the total magnetic moment mentioned earlier.

In summary, the phase stability and the magnetic properties of the $B2$ - and the $L2_1$ -type $\text{Co}_2\text{Cr}_{1-x}\text{Fe}_x\text{Al}$ alloy system were investigated. It was confirmed that two-phase separation from the $B2$ phase to the $B2$ and $A2$ phases inevitably takes place in the concentration range less than $x=0.4$, resulting in a deviation of the saturation magnetic moments from the generalized Slater-Pauling line of $M_t=Z_t-24$. In the concentration range more than $x=0.7$, the single phase of the $L2_1$ -type phase is obtainable. However, half-metallic properties can no longer be obtained in this concentration range. In light of the present results, it is proposed that the most favorable concentration for spintronic devices is located around $x=0.4$ in the $\text{Co}_2\text{Cr}_{1-x}\text{Fe}_x\text{Al}$ alloy system having the $B2$ phase. Recently, half-metallic properties of Co_2CrGa in the $B2$ phase have also been reported.²⁴

The authors are very grateful to Professor K. Inomata, Professor M. Shirai of Tohoku University, and Dr. K. Ishikawa of Kitami Institute of Technology for many helpful discussions. R.Y.U. was supported by Research Fellowships of the Japan Society for the Promotion of Science for Young Scientists.

¹R. A. de Groot, F. M. Mueller, P. G. van Engen, and K. H. J. Buschow, *Phys. Rev. Lett.* **50**, 2024 (1983).

²J. Kübler, A. R. Williams, and C. B. Sommers, *Phys. Rev. B* **28**, 1745 (1983).

- ³S. Ishida, S. Sugimura, S. Fujii, and S. Asano, *J. Phys.: Condens. Matter* **3**, 5793 (1991).
- ⁴S. Ishida, D. Fujii, S. Kashiwagi, and S. Asano, *J. Phys. Soc. Jpn.* **64**, 2152 (1995).
- ⁵I. Galanakis, P. H. Dederichs, and N. Papanikolaou, *Phys. Rev. B* **66**, 174429 (2002).
- ⁶H. J. Elmers, G. H. Fecher, D. Valdaitsev, S. A. Nepijko, A. Gloskovskii, G. Jakob, G. Schönhense, S. Wurmehl, T. Block, C. Felser, P.-C. Hsu, W.-L. Tsai, and S. Cramm, *Phys. Rev. B* **67**, 104412 (2003).
- ⁷T. Block, C. Felser, G. Jakob, J. Ensling, B. Mühling, P. Gütlich, and R. J. Cava, *J. Solid State Chem.* **176**, 646 (2003).
- ⁸A. Kellou, N. E. Fenineche, T. Grosdidier, H. Aourag, and C. Coddet, *J. Appl. Phys.* **94**, 3292 (2003).
- ⁹S. Ishida, S. Kawakami, and S. Asano, *Mater. Trans., JIM* **45**, 1065 (2004).
- ¹⁰Y. Miura, K. Nagao, and M. Shirai, *J. Appl. Phys.* **95**, 7225 (2004).
- ¹¹Y. Miura, K. Nagao, and M. Shirai, *Phys. Rev. B* **69**, 144413 (2004).
- ¹²I. Galanakis, *J. Phys.: Condens. Matter* **16**, 3089 (2004).
- ¹³K. Inomata, S. Okamura, R. Goto, and N. Tezuka, *Jpn. J. Appl. Phys., Part 2* **42**, L419 (2003).
- ¹⁴S. Okamura, R. Goto, N. Tezuka, S. Sugimoto, and K. Inomata, *Jpn. J. Appl. Phys., Part 1* **28**, 172 (2004).
- ¹⁵K. H. J. Buschow and P. G. van Engen, *J. Magn. Magn. Mater.* **25**, 90 (1981).
- ¹⁶J. Kübler, *Physica B & C* **127**, 257 (1984).
- ¹⁷I. Ohnuma, R. Kainuma, and K. Ishida (unpublished).
- ¹⁸K. Ishikawa, M. Ise, I. Ohnuma, R. Kainuma, and K. Ishida, *Ber. Bunsenges. Phys. Chem.* **102**, 1206 (1998).
- ¹⁹H. J. Elmers, S. Wurmehl, G. H. Fecher, G. Jakob, C. Felser, and G. Schönhense, *Appl. Phys. A: Mater. Sci. Process.* **79**, 557 (2004).
- ²⁰A. Yamasaki, S. Imada, R. Arai, H. Utsunomiya, S. Suga, T. Muro, Y. Saitoh, T. Kanomata, and S. Ishida, *Phys. Rev. B* **65**, 104410 (2002).
- ²¹P. J. Brown, K. U. Neumann, P. J. Webster, and K. R. A. Ziebeck, *J. Phys.: Condens. Matter* **12**, 1827 (2000).
- ²²S. Picozzi, A. Continenza, and A. J. Freeman, *Phys. Rev. B* **66**, 094421 (2002).
- ²³I. Galanakis, *Phys. Rev. B* (in press).
- ²⁴R. Y. Umetsu, K. Kobayashi, R. Kainuma, A. Fujita, K. Fukamichi, K. Ishida, and A. Sakuma, *Appl. Phys. Lett.* **85**, 2011 (2004).